10TH INTERNATIONAL SYMPOSIUM ON PARTICLE IMAGE VELOCIMETRY – PIV13
Delft, The Netherlands, July 1-3, 2013

Robust clinical cardiac Echo Particle Image Velocimetry (EchoPIV)

Brett Meyers[1], John Charanko[1], Min Pu[2], William Little[2] and Pavlos Vlachos[1]

[1] Department of Mechanical Engineering, Virginia Tech, Blacksburg, Virginia

bam42@vt.edu

[2] Wake Forest University Baptist Medical Center, Cardiology Center, Wake Forest, North Carolina

ABSTRACT

Heart disease is one of the primary causes of morbidity and mortality throughout the world and non-invasive imaging modalities such as echocardiographic ultrasound and magnetic resonance imaging (MRI) are often used for diagnosis or to guide treatment. However, these methods either provide limited insight into fluid dynamics (ultrasound) or are slow and expensive (MRI). Echo Particle Image Velocimetry (Echo-PIV) is a developing diagnostic approach with the potential to overcome limitations of current methods, providing good spatial and temporal resolution information for improved understanding of cardiac flows. Although showing promise, a minority of the current literature has presented analysis of clinical data, and only in a research setting, not routine clinical practice, since use of contrast agents is only clinically indicated for subjects with poor ultrasound image quality. This restriction makes use of Echo-PIV on these patients difficult. To overcome the limitation imposed by image quality in routine clinical scans, we propose the use of short-time moving window ensemble (MWE) methods to improve signal-to-noise (SNR) ratios while preserving the instantaneous fluid mechanics of the results. In addition to traditional summed correlations, we also implemented a product of correlations (PoC) ensemble method to further increase correlation SNR. Tests were conducted on a cohort of 14 patients for whom the use of ultrasound contrast agent was clinically indicated, and the quality of the resultant vector fields was compared between instantaneous cross correlation and the two new ensemble methods. For single frame measurements with standard cross correlation, only 43% of the vectors were likely to be reliable with peak ratios (PPR) over 2.0, while about 90% of both ensemble methods had PPR > 2.0, slightly higher for the PoC. Using frame-to-frame velocity difference as a proxy for random error, the standard deviation of velocity difference was at least twice as large for the instantaneous correlations as for MWE. Qualitative examination of the flow fields showed vectors fields that were more physically plausible, with fewer areas of apparent loss of correlation and better agreement with color M-mode scans (CMM). Finally, in comparison to clinically measured inflow velocities from mitral inflow Doppler and CMM ultrasound, fits of echo-PIV values showed lower RMS error and higher R2 values for MWE than for the single-frame correlations. In conclusion, moving window ensemble in conjunction with a product of correlation method demonstrates the ability to provide credible velocity information throughout the heart cycle even in routine clinical scans with low SNR for which traditional instantaneous correlation methods largely fail to resolve the flow physics.

INTRODUCTION

Heart disease is one of the primary causes of morbidity and mortality throughout the world., and non-invasive imaging modalities such as echocardiography and magnetic resonance imaging (MRI) are often used for diagnosis and in the course of various treatments for it. These tools provide means to view physical abnormalities as well as measure blood flow and tissue velocities. Several post-processing techniques, developed specifically for these modalities, provide measures for stress/strain and pressure gradients, information which until recently could only be determined by invasive procedures and surgery [1-4].

These practices are limited, however, providing little or no information of the fluid dynamics. Echocardiography velocity measurement techniques implement the use of a thin, linear scan line, producing a single dimensional data vector obtained from the transducer axial direction. Computational and operational costs make MRI difficult to use and justify, despite the fact that it can provide increased spatial information allowing the entire region of interest to be viewed with high resolution. Echo Particle Image Velocimetry (Echo-PIV) is a developing approach with the potential to overcome limitations presented by current methods, providing higher order spatial information with high temporal resolution for improved understanding of cardiac flows.

Echo-PIV is an evolving innovation in the PIV community, ushered in during the early part of the last decade when the first applications focused on the study of patient-specific complex carotid artery models from image scans [5]. Sengupta et al. was the first to demonstrate the feasibility of using Echo-PIV in cardiac medicine [6]. Through the use of ultrasound contrast agents, previously reserved for improving tissue identification, 2-dimensional flow could be

visualized. Research utilizing this technique has expanded, encompassing experiments to assess flow structure formations and effects due to congestive heart failure (CHF) progression, optimization of techniques to provide more robust results, determination of other limiting factors (i.e. under sampling and bias error), and extreme cases of heart disease and deformities such as Fontan hearts [7-9].

At present less than one third of the EchoPIV literature has concentrated on the analysis of clinical data, indicating that Echo-PIV has yet to reach a point of accepted use within the medical community [7, 9-11]. Issues with image quality severely limit the ability for accurate PIV measurements, and Echo-PIV is no exception, since clinically indicated use of contrast agents is primarily on subjects with poor image quality scans. An example image for a typical patient is shown in Figure 1 alongside an example from Sengupta's original cardiac work [6]. Image quality and seeding density appear to be starkly different between these two individuals. As a result, any clinical study tends to be comprised of "optimal" cases. This further inhibits the acceptance of Echo-PIV in the cardiac community due to the biased sample population from which data is derived [11]. Although optimum acquisition parameters have been determined, clinical scan quality can still be inadequate, thus requiring the development of processing strategies to overcome these limitations [8].

Figure 1: Comparison B-Mode images between (Left) an average patient from clinical scans and (Right) an image provided from Sengupta's online supplemental material [6]

Several approaches have been proposed to improve Echo-PIV cross-correlation processing. These works focus on *in-situ* algorithms that aim to amplify the true correlation peaks, improve peak detection, identify and remove outliers, and reconstruct the flow field based on conservation laws [12-15]. However these methods are based on corrections for steady flows, which is not the case for cardiac flows. As an alternative approach, ensemble techniques offer a method to converge the measurement onto a mean, representative solution. A small number of papers focus on the use of ensemble methods to improve correlation strength and allow for the true peak to be identified, but these, too, focus on application to steady flow systems [15]. Nevertheless ensemble methods could be used on cardiac Echo-PIV to obtain velocity measurements that are potentially more robust and accurate. Hence, we hypothesize that developing and using short-time moving ensemble correlation methods through the combination of 3 to 5 planes can produce near-instantaneous flow measurements of time-varying flows with improved accuracy and robustness for EchoPIV applications.

This work will present methods to overcome noise and recording limitations, improving EchoPIV results and applicability. The methodology development and application processes presented here will further substantiate the necessity for improved image processing capabilities. Qualitative and quantitative validation on clinical patient data will serve to demonstrate the robustness and accuracy of these techniques.

METHODOLOGY

EchoPIV Development Cohort

The patient cohort for this work was provided by the Cardiology Center at Wake Forest University Baptist Medical Center in accordance with IRB 08-057 approved protocol using iE33 ultrasound image systems. All patients were admitted for routine echocardiography procedures, and were included in the study based on the clinically indicated need for contrast agent injection. Exclusion criterion for this work was imposed on individual scans, observing seeding density; data sets with very low seeding were excluded. Subjects from this study suffered from heart failure, however the degree/stage of disease progression was not considered. A total of 14 patients were analyzed, with information about the patient cohort is provided in Table 1.

Table 1: Cohort Clinical Information Breakdown

Clinical Procedure	Gender (Total/Female)	Age (Yrs) (Average, Min/Max)	E/A	E/e'	B-mode scans (Total Per Sub-Cohort)
Mitral Inflow	9/3	62.4 (32/75)	1.16	10.3	23
Color M-mode	7/3	58.7 (33/78)	1.19	-	17

B-mode echocardiogram scans were performed capturing 2-D views of the heart in two, three, and four chamber views. Each scan region-of-interest (ROI) was narrowed to contain only the left ventricle, from the apex to the mitral annulus, providing the best spatial resolution for analysis. The trade-off for this specific view comes at the cost of temporal resolution. Average frame rates for this cohort group were approximately 120 fps. All scans contained a minimum of two cycles (beats). Additional scans were performed, including Doppler mitral inflow measurements and Doppler Color-M-Mode echocardiograms, which can be used independently to measure patient blood flow velocities along a scanline. These two methods represent the most widely used clinical modalities for measuring blood flow in the heart and will be used herein for quantitative comparisons to the corresponding EchoPIV results. Further breakdown for specific patient information, including data from Mitral Inflow and Color M-mode, is provided in Table 2.

Table 2: Individual Scan Information for Sub-Cohort Structure

Patient	Scans	MI (Y/N) (E/A [cm/s])	CMM (Y/N) (E/A [cm/s]))
1	1	Y (63.2/99.7)	N
2	3	Y (98.7/50.8)	N
3	3	Y (83.4/69.6)	N
4	3	Y (60.7/81.9)	N
5	4	Y (50.3/57.3)	N
6	3	Y (85.4/82.9)	N
7	2	Y (119/71.1)	N
8	3	Y (66.0/51.0)	Y (77.7/57.9)
9	1	Y (99.2/76.5)	Y (61.4/41.9)
10	1	N	Y (62.9/52.0)
11	4	N	Y (59.5/74.4)
12	3	N	Y (76.4/45.9)
13	3	N	Y (77.7/56.8)
14	2	N	Y (50.6/58.2)

Mitral Inflow (MI) scans are displayed in a histogram-type format of velocity versus time with the strength of the signal at each velocity expressed as intensity. A representative MI plot reconstructed based on EchoPIV data is shown in Figure 2. Peak velocities for early and late diastolic filling stages are found by selection of the peak velocity observed at the tip of the respective filling peak. Color M-mode (CMM) displays information in a spatiotemporal format, with velocities expressed as color changes on a contour map, with a clinical example image also shown in Figure 2. Due to limitations of the Doppler format, velocities are constrained to a limited range and velocities higher or lower are aliased cyclically to the opposite extreme. Typically, lab technicians will adjust the aliasing boundary to assist in visualizing the shape of the early filling contour, causing the maximum filling velocities to be reported as negative values (blue regions in the CMM scan in Figure 2). Peak velocities are taken from this map through de-aliasing the contour and searching for the peak contour value. These measurements were performed using the Color M-mode software package developed by the AEThER Lab [16]

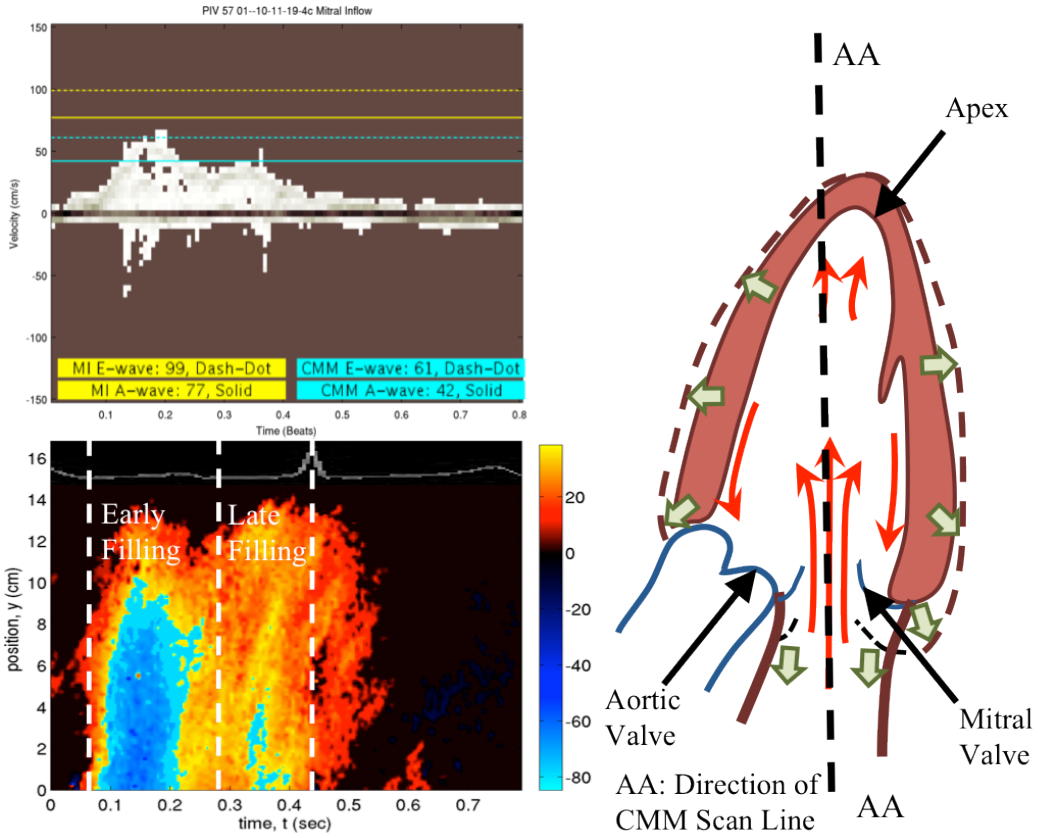

Figure 2: Examples of blood Doppler measures in echocardiography. These two methods are (Top Left) Mitral Inflow, a histogram measure, and (Bottom Left) Color M-mode, a spatiotemporal contour measure. Both methods scan from the Mitral Valve to Apex, as shown in the example illustration (Right).

PIV Processing

To provide a baseline for comparison of the new methods proposed here, Standard Cross-Correlation (SCC), the current standard for processing EchoPIV derived particle images, and the Robust Phase Correlation (RPC), a method developed for optimized energy phase filtering to improve correlation [17, 18] are used. Each of these PIV processing strategies, along with the ensemble methods, were performed on the B-mode image sets through the use of a customized version of the PRANA PIV suite, developed by the AEThER Lab at Virginia Tech [19]. Further details of the ensemble correlation techniques are provided below.

Moving Window Ensemble Correlation

Ensemble-averaging correlation, which was first introduced for μPIV applications, is a method used to increase the signal-to-noise ratio (SNR) of the correlation plane [20, 21]. Correlation ensemble schemes are typically applicable only to steady state or time-averaged flows, with little temporal velocity variation, in order to obtain credible results. Given the cohort's echocardiography low frame rates (~ 120 fps or less) and the nature of cardiac flows (periodic and unsteady) it is not appropriate to apply the traditional ensemble correlation to perform cardiac Echo-PIV. However, here we propose the use of a moving window ensemble (MWE) correlation to allow the capture of robust, near instantaneous flow measures. An example of this architecture difference is depicted in Figure 3.

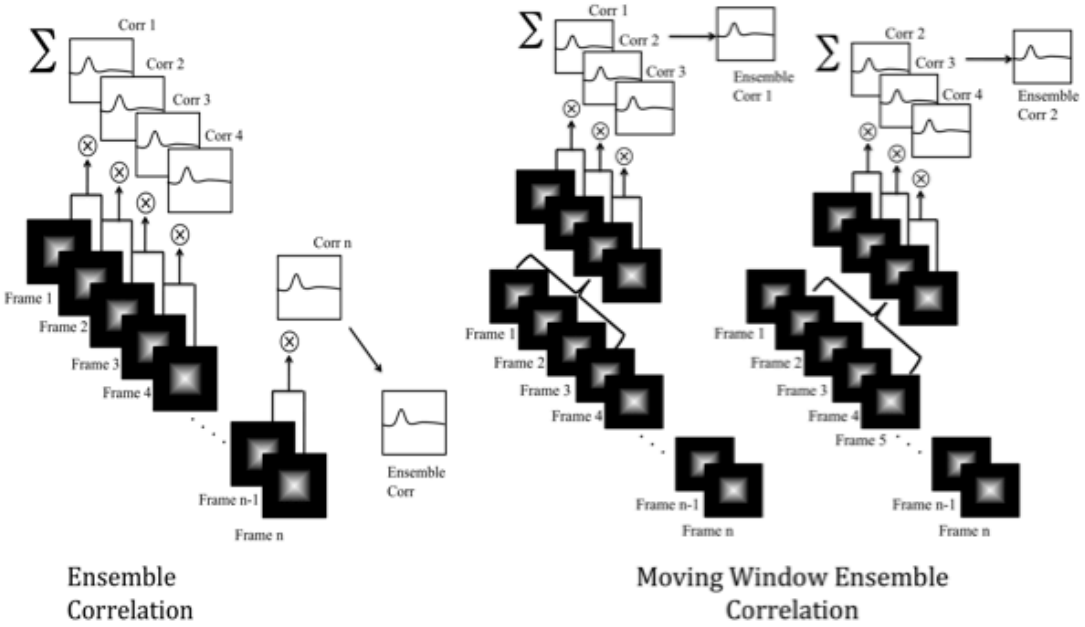

Figure 3: Example of Ensemble Correlation (Left) versus MWE Correlation (Right). Using a short series of images for specific applications, such as unsteady flows, can provide a means of obtain accurate results on low SNR images.

Ensemble based on Sum of Correlation

The MWE methodology, infrequently performed in PIV applications, implements the use of a short-time ensemble series to resolve the flow from noisy data that cannot produce clear, robust instantaneous measures [22]. The MWE works to suppress image noise, increasing SNR over the small subset for more accurate velocity predictions. Standard ensemble averaging and MWE schemes implement an arithmetic mean, where all terms in the set are summed together and scaled, in order to find a suitable average for the data being analyzed. This method, herein referred to as Sum of Correlation (SoC), is described mathematically below.

$$\overline{R}(s)_j = \sum_{i=j}^{j+N-1} R(s)_i \tag{1}$$

The performance of the SoC method is dependent on the condition that all correlation planes have a common mode that is consistently strong at or near a constant displacement. Still, limitations on performance arise from the amount of erroneous correlated noise. If noise dominates the correlation, with random noise having shared common peaks with relative high intensity in most frames, a SoC method-based MWE can fail.

Ensemble based on Product of Correlation

Through the use of a geometric mean as a secondary approach to data averaging, MWE correlation can yield improved robustness in comparison to the traditional measures. In this scheme the correlation planes are multiplied together, allowing only consistent high-level correlation values to exist within the plane. This approach, first conceptualized by Hart in 2000, can significantly increase SNR by filtering out non-overlapping random correlation noise [23]. Furthermore, due to the multiplicative nature of this method, convergence of this scheme allows for the reduction of the number of frames required while providing increased confidence in correct peak detection. This method, referred to herein as Product of Correlation (PoC), is described mathematically below.

$$\overline{R}(s)_j = \prod_{i=j}^{j+N-1} R(s)_i \tag{2}$$

It must be noted that the PoC MWE method is highly sensitive to the presence of overlapping common modes, requiring all signal peaks to be within the same magnitude and direction across each plane. Random noise using this strategy should effectively be filtered out, achieving an exponential SNR increase. This is largely due to the small set size, which decreases the likelihood of high variability between the peak estimates, while ensuring that random noise should not have significant overlap across the set planes.

Processing Set-up

All cases were processed using a single-pass correlation scheme. The rationale behind this stems from the notion that EchoPIV results should show good correlation in the first pass in order to be acceptable. Subsequent passes provide only refinements of the initial velocity estimation. Physical window sizes are 128 x 128 pixels with effective resolution of 48 x 48 pixels using a Gaussian apodization function [18]. These parameters are selected based on physical pixel width and height for the ROI, and the velocity at which the contrast agents will be moving within the region. Application of the RPC method requires knowledge of the flow tracer diameter, established for this work as an average size of 7 pixels. Ensemble sizes for both SoC and PoC methods were restricted to 3 correlation planes, in order to limit underestimation effects introduced by the averaging.

Post-processing and analysis

Processing results across each technique were tested through several qualitative and quantitative comparisons. The first qualitative approach analyzed vector fields and vorticity to compare typical flow characteristics seen in the left ventricle of the heart. Particular attention was paid to the physical consistency of the results between consecutive frames. Vorticity was calculated using a second-order central finite difference scheme. The second qualitative approach focused on creating spatiotemporal velocity contour maps along a line extending from the mitral valve to the apex versus time from the EchoPIV vector fields, providing means for a direct comparison to the clinical CMM. The contour maps were evaluated for similarity to CMM, specifically for their ability to capture the basic physiology of the heart cycle in terms of velocity magnitude and spatial distribution over time during ventricular filling.

Quantitative metrics to reflect the improvements of the proposed strategies used information from the correlation planes and vector fields to establish measures for reliability and measurement quality. Detectability of the correct displacement peak in the EchoPIV correlation plane for each processing strategy was tested by finding the Peak-to-Peak ratio (PPR) for each measurement, calculated by dividing the height of primary correlation peak by the height of the second largest peak [24]. Although there is not a direct link between the peak ratio and the error of any given measurement, correlations with peak ratios close to one have low signal to noise ratios and are more likely to have failed or have high errors. Previously, Keane and Adrian have stated that any measurement with a peak ratio less than 1.2 has a high likelihood of being a false correlation [24], and Hain and Kähler have suggested that correlations with peak ratios above 2.0 can likely be assumed to be correct [25]. In addition, Charonko and Vlachos demonstrated that for standard PIV processing and the RPC correlation method there is a direct correspondence between the peak ratio and the uncertainty of given measurement [26].

Consistency was investigated through a difference measure based on a temporal continuity assumption. Since the data available is produced from clinical scans, the true velocity values are not available to assess the error of any particular velocity measurement. Instead, this approach is based on the assumption that consecutive frames should only vary gradually in time if the sampling rate is much greater than the patient heart rate. Higher rates of change in the velocity from frame-to-frame likely indicate increased random error in the correlation, or a decreased valid vector percentage (since failed correlations will return random velocities unrelated to the adjacent frames). However, using this approach, increased error could only be estimated relative to other methods, and not in an absolute sense.

Finally, peak EchoPIV velocities for early and late filling stages were compared to Mitral Inflow (MI) and CMM peak values. Each modality was compared to EchoPIV using a least squares linear regression, and the L2-norm of the difference between the EchoPIV peak filling velocity and the clinically evaluated values from MI and CMM. The L2 -norm was calculated as:

$$L_2 = \frac{1}{N}\sqrt{\sum_{i=1}^{N}(x_i - X)^2} \tag{3}$$

Peak EchoPIV velocities were determined by searching spatial regions centered at the mitral valve during both diastolic filling phases, similar to the way MI velocities are sampled clinically. This region was constrained to a spatial window of 11 x 11 vectors in size, and the maximum value was extracted at each time instant during filling cycle. This new data vector of spatial peaks in time was then used to find the final peak inflow velocity during the early and late filling. An example of this procedure is shown in Figure 4.

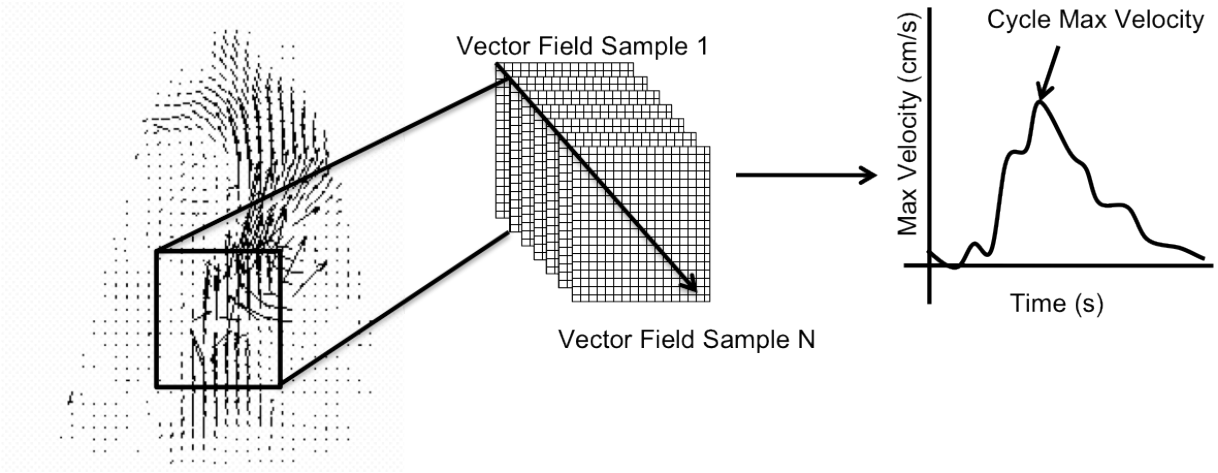

Figure 4: Schematic of procedure for finding the peak velocity during one phase of the diastolic cycle. After correlation (Left) an 11 x 11 spatial window was applied to the frame. The content of this window were then used with the content of all the other frames in the series (Middle) and the maximum for each snapshot was found to construct a new temporal data vector (Right). This vector was then used to determine the maxima in time for comparison with other clinical modalities.

Results

Qualitative analysis of the whole vector fields will focus on the early stage of diastolic filling, requiring a simple overview of the basic cardiac mechanics involved. Diastolic filling occurs after the left ventricle (LV) has contracted and ejected blood out into the body through the aortic valve. Diastole is the longest portion of the cardiac cycle, taking up approximately 2/3 of the entire process. As the LV relaxes during the early portion of filling, blood flow crosses the mitral valve and a high velocity jet forms and is responsible for moving most of the blood from the atrium into the ventricle. This jet forms a vortex ring near the leaflets of the mitral valve, and later in the cycle the filling wave reaches the apex of the heart and a recirculation region forms preserving the momentum of the blood flow. Afterwards, the left atrium contracts, expelling a second late filling wave into the LV with similar jet and vortex ring dynamics, and completing the filling of the heart in preparation for systolic contraction of the LV and the ejection of blood into the aorta.

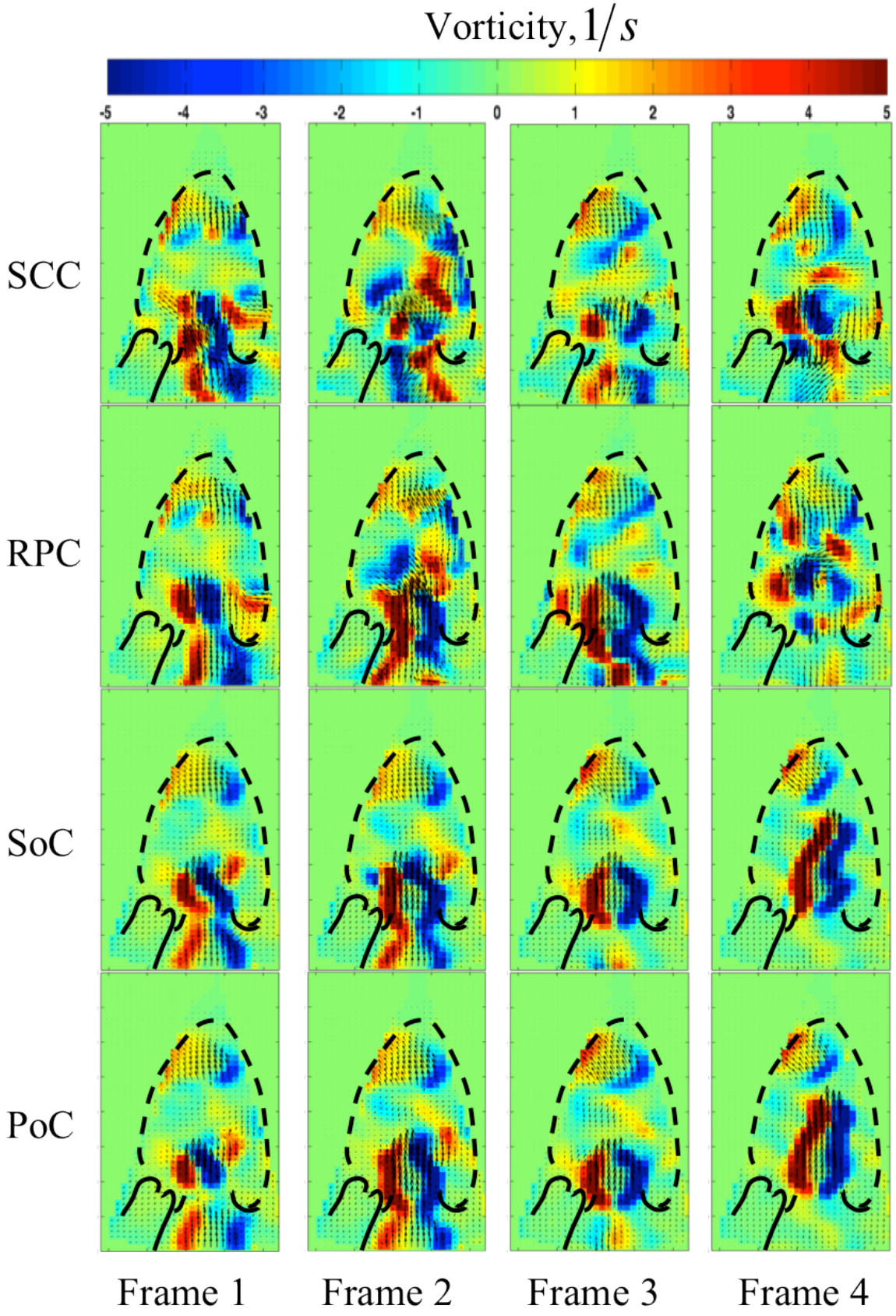

Figure 5: Early diastolic inflow comparison for SCC, RPC, SoC and PoC correlation strategies. During inflow, the blood passes through the mitral valve, generating a region of high shear as it enters, shown through the vorticity contour field.

A representative patient from the original cohort, with both MI and CMM information, was selected for use in qualitative comparisons. Consecutive vector fields overlaid with vorticity contours for the representative patient are shown in Figure 5. These fields are illustrative of the reliability and accuracy of clinical EchoPIV measurements based on the recorded scan during this study. Instantaneous measurements (SCC and RPC) initially captured the diastolic inflow jet (Frame 1), shown on the vorticity as a large shear region near the base of the image. In successive fields SCC produced many non-physical behaviors, such as rapid development and disappearance on velocity in the ventricle between sequential frames (Frames 2-4) and regions that showed reversed flow back toward the atrium at the bottom of the scan instead of a strong upward filling jet. Other regions of apparent disorganized flow were also seen where smoothly varying velocity fields in space and time were expected. These types of behaviors were likely attributable to loss of correlation due to low seeding densities or very high velocities. The RPC method better resolved the large shear region through the valve, but failed to correlate when the jet had fully penetrated into the ventricle (Frame 4), resulting in a very disorganized and non-physical field. It also showed evidence of the same loss of correlation in the peak flow region of the jet as was seen in the instantaneous SCC results. For the ensemble methods (SoC and PoC), a full and continuous natural flow behavior was produced with little evidence of the loss of correlation seen from the two instantaneous methods. Here we saw that the shear region crossing the mitral valves passed from the atrium to the ventricle and began to progress towards the apex. This image series clearly showed the benefits of short time ensemble processing strategy on clinical patient data.

In Figure 6 one can immediately see the increased ability for SoC and PoC measures (c & d, respectively) to better approximate clinical results seen from CMM (e). Results from SCC (a) and RPC (b) have high noise, barely capturing the shape of the jet inflow region (leading deep blue region shown in (a), ~0.1 seconds). This blue region is the period of maximum inflow, and it can be seen that many of the values there and throughout the cycle are near 0, indicating a loss of correct correlation and most likely an incorrect correlation with stationary background noise or structures. Ensemble strategies conversely generate regions that closely match the CMM region properties, although they still struggle to fully resolve the peak inflow values at every time instant.

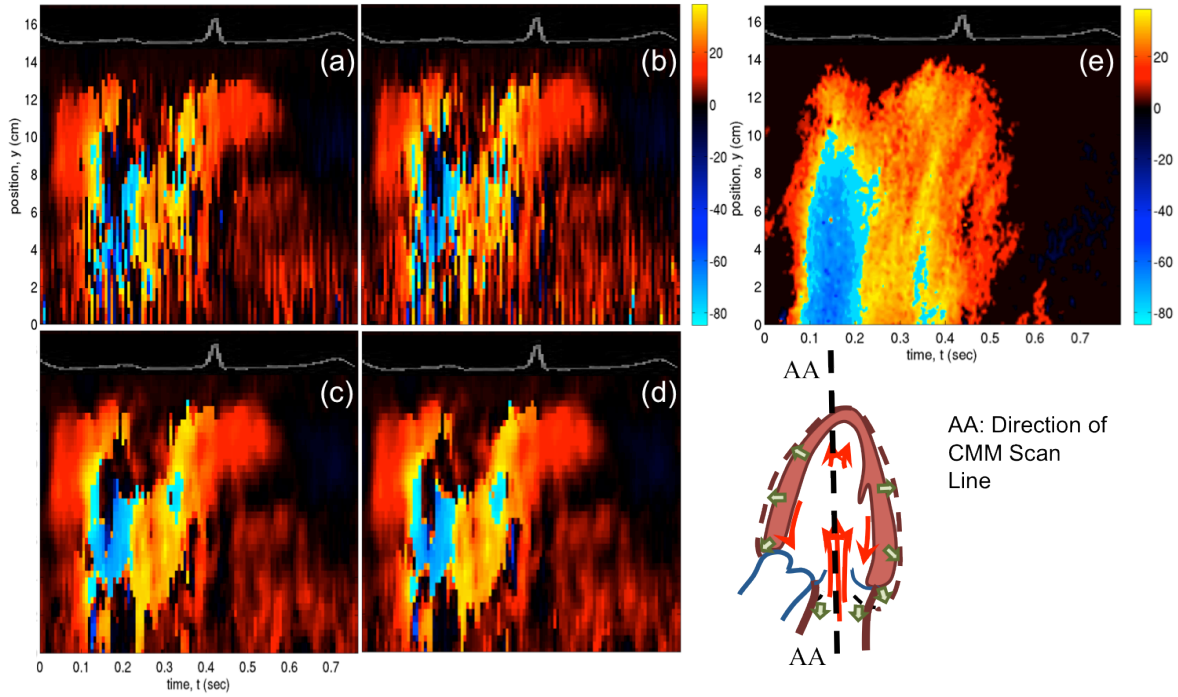

Figure 6: Qualitative comparison of EchoPIV to Color M-mode using a scan-line contour view of the vector field. Processing strategies are for (a) SCC, (b) RPC, (c) SoC, and (d) PoC are shown side-by-side with (e) the patient clinical contour map.

Quantitative measurements of the PPR are shown in Figure 7, but required normalization of the ensemble methods to allow a fair comparison between all processing schemes. Due to the summation, the correlation plane values for SoC were on average 3 times higher than for an instantaneous measurement taken under similar conditions. The PoC was larger by the cube of the typical value due to the multiplication of the planes. To reverse these effects the SoC values were divided by three and the cube root of the PoC peak ratio was performed.

Observing the information provided from the CDF calculations, it is determined that SCC had just under 20% of all PPR values within a range of 1 to 1.2. In contrast, the RPC method only contained approximately 10% of all vectors, while both ensemble methods had less than 3% PPR within the same nominal range. Previous work has suggested that

an acceptable range for a valid peak detection starts at a PPR of 1.2 [24]. This information suggested that only about 80% of the SCC vectors had been properly detected, a significant difference in comparison to the 97% for the ensemble methods.

Furthermore, if a PPR of 2 is used as the minimum threshold for valid detection [25], the SCC had just 43.29% of measurements above this value. Through this metric the RPC had 70.55% reliable vectors, while the SoC and PoC had 89.77% and 90.43%, respectively, suggesting that the PoC had slightly better detectability than the SoC.

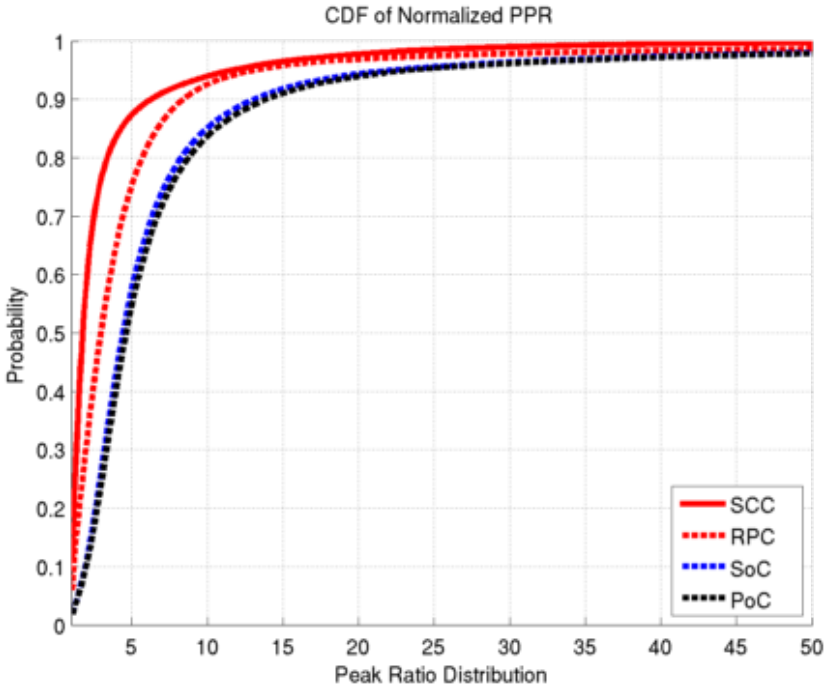

Figure 7: Cumulative Density Functions (CDFs) of Peak-to-Peak ratio (PPR) for every vector and processing method. Curves up and to the left indicate lower average PPR and thus potentially less reliable correlation data.

Table 3: Peak-to-Peak Ratio Statistics for processing methods

Process	Probability under PPR 1.2 (x 100)	Probability over PPR 2 (x 100)
SCC	18.48	43.29
RPC	9.41	70.55
SoC	2.51	89.77
PoC	2.46	90.43

The CDFs of the frame-to-frame velocity differences (Figure 8) serve as a means to quantify the amount of variation that occurs specific to that processing strategy. In essence, the frame-to-frame differences are reflected as accelerations observed in the flow. As a point of reference, an average of 0.03 cm spatial resolution is present in a typical scan with a time step of 0.008 s between frames, so a change per frame of one pixel/frame of velocity yields an approximate acceleration of 3.75 cm/s per frame. Observations from the ensemble measures indicate that most accelerations in the flow are gradual, and only a minimal amount of high values are present and the majority of these accelerations are only present during the high velocity regimes (i.e. during inflow). Because the distributions are not perfectly Gaussian and have long tails, examination of the standard deviations alone does not provide sufficient information for an accurate comparison between methods. Instead, by observing the 5%/95% thresholds it can be established that nearly all the differences from the ensemble method fall below this single pixel acceleration. By contrast the 5%/95% ranges on the instantaneous measures are consistently double this on both U and V velocities. These threshold values typically show approximately 9 cm/s difference between frames; from our data a peak velocity of 40-80 cm/s is typically observed, for a 10-20% difference frame-to-frame as compared to the maximum velocity measured. Additionally, the tails on the

CDF curves for instantaneous measures are fat, further suggesting that calculated accelerations for the instantaneous measure are often much greater than a 10% difference per frame at least 10% of the time, which is, given the acquisition parameters and physics of the system, not realistic. Put another way, on average the frame-to-frame variance was twice as large as for the instantaneous methods compared to the MWE methods, with the difference likely due to increased random error and decreased fraction of valid vectors for the instantaneous methods.

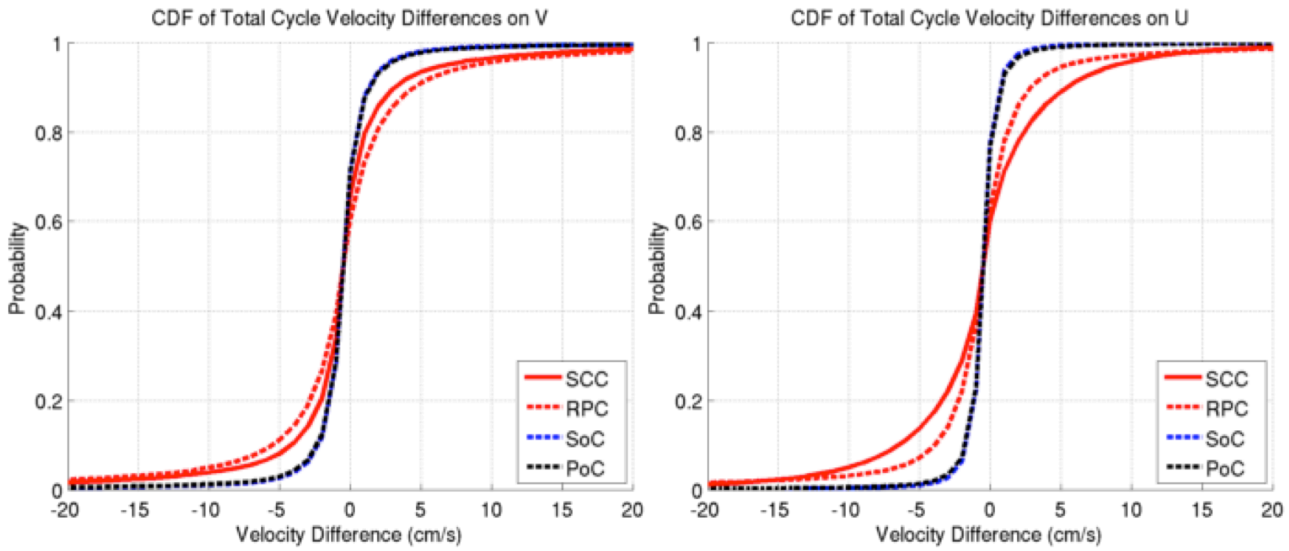

Figure 8: CDFs for the temporal variance associated with each processing method on V and U. Consistent behavior is seen for the ensemble measure. SCC behavior performed better on V but not on U, indicating the inability to resolve properly any spatial forms such as rotation. RPC performs poorly overall.

Table 4: Statistical information for Velocity Difference

Method	Difference on V		Difference on U	
	5% / 95% (cm/s)	2σ (cm/s)	5% / 95% (cm/s)	2σ (cm/s)
SCC	-9.1/7.21	5.11	-11.31/-9.27	4.63
RPC	-11.1/9.19	6.26	-7.63/5.63	4.69
SoC	-4.64/2.70	2.73	-3.44/1.44	1.56
PoC	-4.77/2.83	2.97	-3.62/1.61	1.81

Direct comparison of the EchoPIV velocity measurements to MI Doppler scans (Figure 9) indicated that matching of peak velocities for all methods of EchoPIV was not possible; there was a bias difference present for all cases. This difference was most pronounced for the SoC method. Differences between the PoC and SCC processing methods were small, but the scatter in the means of all patients and the case-to-case deviations for a single patient with the SCC were much more pronounced. The RPC method has the best line fit, but has the worst scatter of data to produce this trend.

The bias difference between these two modalities may have resulted from undersampling by B-mode Echocardiography, as has been shown by Gao et al. [8] to result in reductions in the peak velocities measured. Conventional B-mode images have a typical maximum frame rate of 150 Hz. In comparison, the MI and CMM methods at their lowest sweep speeds still have sampling rates above 200 Hz.

The coefficient of determination, or correlation, R^2, can provide insight into the accuracy of the methods. Although the SoC method produces the largest slope for the data fit, the coefficient for this method is strongest, with a value above 0.549. The PoC method produces a similar scatter behavior to the SoC, with a slightly lower R2 value but with a slope closer to 1:1 and a smaller intercept. This suggests that although all methods express a bias, the PoC processing offers the best trade-off of un-biased peak velocities and lower scatter in the results.

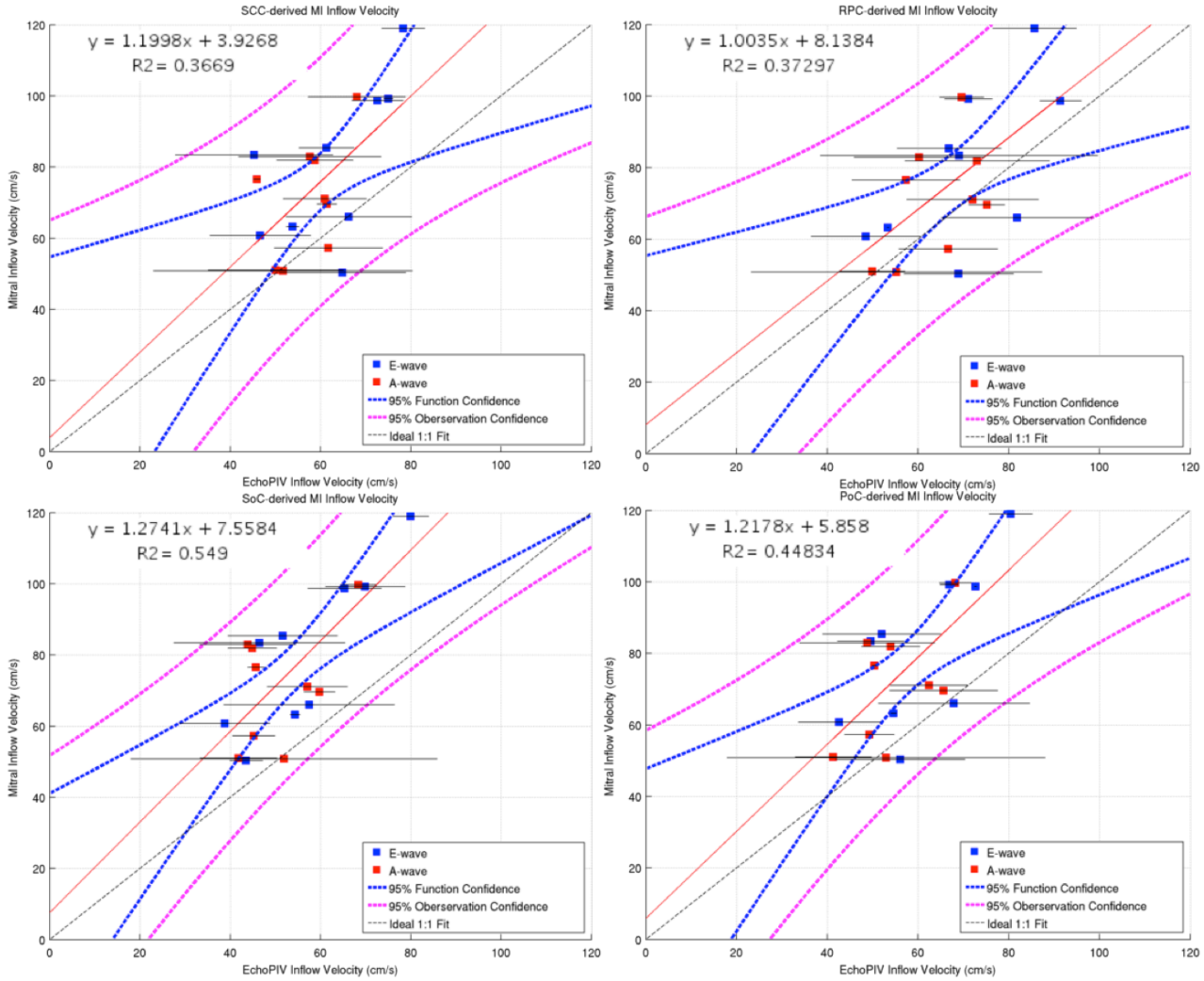

Figure 9: MI to EchoPIV velocity comparison. Scatter trend lines indicate the fit of the EchoPIV velocities to MI velocities for early filling (E-wave) and late filling (A-wave) during diastole.

Comparisons of the EchoPIV peak velocities to the CMM (Figure 10) produce very similar results to the ones from the MI trends. The bias for each method is similar in magnitude to the MI cases, but the slope of the linear regression fits are nearly reverse, suggesting that the EchoPIV measures are larger than the CMM-derived values. However, the larger intercept values counteract this trend, leading to EchoPIV results that are grouped around the 1:1 line over the range of measured cases. The only exception is the RPC instantaneous results where the values are consistently higher than the 1:1 line. The R^2 values for the fits for the SoC and RPC methods show a slightly lower value than what was previously seen in the MI, however the linear fit slopes for the data have a larger divergence from the 1:1 fit. The PoC and SCC techniques remain near the same value for CMM, with the slopes for each method remaining within close proximity to the ideal fit. This allows us to conclude that, through data scatter, R^2, and slope, the PoC processing method provides measurements that, for the present cohort, are near the CMM measurements with more reliability than that of the other methods.

Measurements for the total error of each processing case are provided through the L2 norm calculations, pictured in Figure 11 with averages over all the samples for each processing method tabulated in Table 5. We observe that all methods have relative similar L2 Norms. Looking at each method's mean L2 value, it can be seen that the SoC method has the largest L2, agreeing with the initial assessment made when observing the MI plots. Although the means for the instantaneous cases are lower, the behavior of the RPC method has a slightly larger variance. Overall, the L2 norms for each comparison only varies at most by 2 cm/s across each method, while the difference in the errors between MI and CMM is only 7 cm. These comparison measures overall, suggest that there is a case for comparison to be made, but limited data prevents a conclusion from being made.

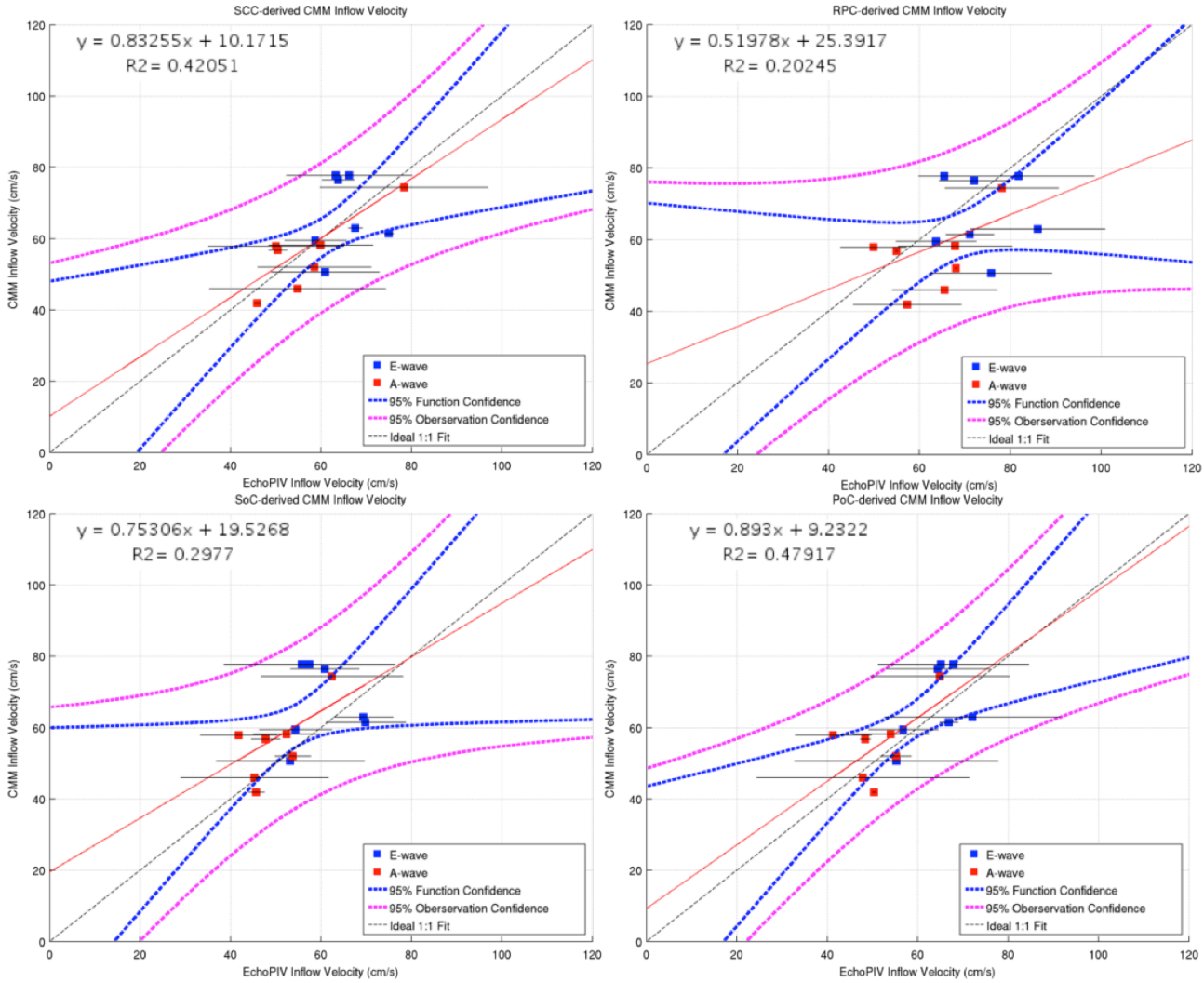

Figure 10: CMM to EchoPIV velocity comparison. Scatter trend lines indicate the fit of the EchoPIV velocities to CMM velocities for early filling (E-wave) and late filling (A-wave) during diastole.

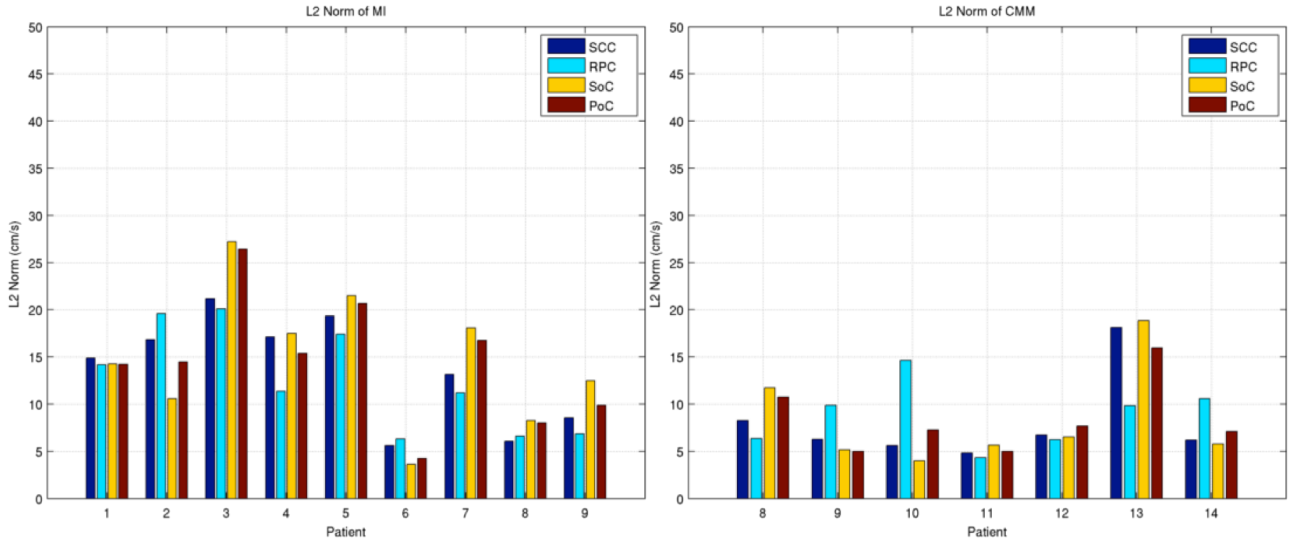

Figure 11: L2 Norm plots for expressing average bias error for EchoPIV in comparison to (Left) MI and (Right) CMM clinical modalities.

Table 5: Mean L2 Norm Values of each processing method for MI and CMM comparison modalities

Method	MI (cm/s)	CMM (cm/s)
SCC	13.25	8.00
RPC	11.75	8.84
SoC	15.19	8.23
PoC	14.24	8.38

DISCUSSION AND CONCLUSIONS

EchoPIV, in its current state, is an emerging and developing tool for clinical research applications, but has shown very limited applicability on clinical data. Qualitative results showed that the traditional PIV processing provides a very inconsistent ability to properly resolve the flow fields, which leads to discrepancies when comparison is made to other modalities such as a CMM contour map. Furthermore, the quantitative measures for PPR and Velocity Difference re-enforce the conclusion that data from this method are unreliable. If the suggested criterion by Hain and Kahler were applied (PPR greater than 2 should be correct), the majority of vectors calculated (60%) should be considered as unreliable.

In contrast, the ensemble methods through qualitative and quantitative results strongly suggest that they provide significant improvement. Observations made from the vector fields indicate that the ensemble approaches resolve the high velocity jet that travels from the atrium into the ventricle, matching what is previously known about the flow physics in the ventricle. Comparison to the CMM contour map in this study also shows an overall improvement in resolving the appropriate velocity and matching the behavior of the cycle to a much better degree. Results from PPR indicate that the ensemble methods are roughly 5 times more reliable.

Even with all of this information determined, the comparison of peak velocities from EchoPIV to MI and CMM modalities end up providing results that do not re-enforce the early results. Bias differences from between EchoPIV and MI are very pronounced; shifting all linear regression fit slopes above the ideal 1:1 line. It is speculated that this bias may be due to the sampling rate differences between B-mode and Doppler methods, but the CMM fits do not support this conclusion. All methods through this comparison have a very low bias, with the current clinical modality and our proposed PoC strategy providing the best matching to the 1:1 line. One possible explanation for this occurrence could stem from the way in which CMM and MI peak measures were obtained. The reported values for MI were taken by the lab technician and reported to our lab, while the CMM peak values were obtained through the use of available software, and values at the peak were averaged with their temporal neighbors to match the resolution obtained through EchoPIV. A more consistent acquisition protocol could improve these comparisons.

Our objective through this work was to develop and implement a moving window ensemble method for Echo-PIV for producing robust and accurate results on clinical data. Current methods have mostly been derived for research data, however the clinical community can also benefit by further development of this PIV-derived tool. Qualitative results suggest significant improvement, resolving well-established flow patterns both spatially and temporally. Quantitative measures dictate that reliability of the proposed method is improved. Comparison of EchoPIV techniques to accepted clinical modalities suggests good accuracy but noise prevents a fair comparison. These elements support that use of a MWE method with Product of Correlation processing has the potential of producing credible, accurate results through the entire cycle, however additional and extensive development and analysis is still required before the method is ready for routine clinical use.

REFERENCES

[1] Yotti, R., Bermejo, J., Antoranz, J. C., Desco, M. M., Cortina, C., Rojo-Álvarez, J. L., Allué, C., Martín, L., Moreno, M., Serrano, J. A., Muñoz, R., and García-Fernández, M. A., 2005, "A noninvasive method for assessing impaired diastolic suction in patients with dilated cardiomyopathy," Circulation, 112(19), pp. 2921-2929.

[2] Mulvagh, S., Quiñones, M. A., Kleiman, N. S., Jorge Cheirif, B., and Zoghbi, W. A., 1992, "Estimation of left ventricular end-diastolic pressure from Doppler transmitral flow velocity in cardiac patients independent of systolic performance," Journal of the American College of Cardiology, 20(1), pp. 112-119.

[3] Buyens, F., Jolivet, O., De Cesare, A., Bittoun, J., Herment, A., Tasu, J. Ä., and Mousseaux, E., 2005, "Calculation of left ventricle relative pressure distribution in MRI using acceleration data," Magnetic resonance in medicine, 53(4), pp. 877-884.

[4] Helle-Valle, T., Crosby, J., Edvardsen, T., Lyseggen, E., Amundsen, B. H., Smith, H.-J. r., Rosen, B. D., Lima, J. o. A., Torp, H., and Ihlen, H., 2005, "New noninvasive method for assessment of left ventricular rotation speckle tracking echocardiography," Circulation, 112(20), pp. 3149-3156.

[5] Kim, H.-B., Hertzberg, J., Lanning, C., and Shandas, R., 2004, "Noninvasive measurement of steady and pulsating velocity profiles and shear rates in arteries using echo PIV: in vitro validation studies," Annals of Biomedical Engineering, 32(8), pp. 1067-1076.

[6] Sengupta, P. P., Khandheria, B. K., Korinek, J., Jahangir, A., Yoshifuku, S., Milosevic, I., and Belohlavek, M., 2007, "Left Ventricular Isovolumic Flow Sequence During Sinus and Paced RhythmsNew Insights From Use of High-Resolution Doppler and Ultrasonic Digital Particle Imaging Velocimetry," Journal of the American College of Cardiology, 49(8), pp. 899-908.

[7] Hong, G.-R., Pedrizzetti, G., Tonti, G., Li, P., Wei, Z., Kim, J. K., Baweja, A., Liu, S., Chung, N., and Houle, H., 2008, "Characterization and quantification of vortex flow in the human left ventricle by contrast echocardiography using vector particle image velocimetry," JACC: Cardiovascular Imaging, 1(6), pp. 705-717.

[8] Gao, H., Claus, P., Amzulescu, M. S., Stankovic, I., D'Hooge, J., and Voigt, J. U., 2011, "How to optimize intracardiac blood flow tracking by echocardiographic particle image velocimetry? Exploring the influence of data acquisition using computer-generated data sets," European Heart Journal - Cardiovascular Imaging, 13(6), pp. 490-499.

[9] Lampropoulos, K., Budts, W., Van de Bruaene, A., Troost, E., and van Melle, J. P., 2012, "Visualization of the intracavitary blood flow in systemic ventricles of Fontan patients by contrast echocardiography using particle image velocimetry," Cardiovascular ultrasound, 10(1), p. 5.

[10] Kheradvar, A., Houle, H., Pedrizzetti, G., Tonti, G., Belcik, T., Ashraf, M., Lindner, J. R., Gharib, M., and Sahn, D., 2010, "Echocardiographic Particle Image Velocimetry: A Novel Technique for Quantification of Left Ventricular Blood Vorticity Pattern," Journal of the American Society of Echocardiography, 23(1), pp. 86-94.

[11] Cimino, S., Pedrizzetti, G., Tonti, G., Canali, E., Petronilli, V., De Luca, L., Iacoboni, C., and Agati, L., 2012, "In vivo analysis of intraventricular fluid dynamics in healthy hearts," European Journal of Mechanics-B/Fluids.

[12] Niu, L., and Zheng, H., "Algorithms for Correcting Velocity Vectors in Ultrasonic Particle Image Velocimetry," Proc. Bioinformatics and Biomedical Engineering, 2009. ICBBE 2009. 3rd International Conference on, IEEE, pp. 1-4.

[13] Qian, M., Yan, L., Niu, L., Jin, Q., Ling, T., Chen, Y., and Zheng, H., "Micro-ultrasound biofluid imaging and multi-component velocity measurement with micro echo particle image velocimetry technique," Proc. Engineering in Medicine and Biology Society, 2009. EMBC 2009. Annual International Conference of the IEEE, IEEE, pp. 451-454.

[14] Yu, W., Qian, M., Niu, L., and Zheng, H., "An Image-Based Method for Real Time Ultrasonic Microbubble Concentration and Velocimetry Quality Evaluation in Echo PIV Technique," Proc. Bioinformatics and Biomedical Engineering (iCBBE), 2010 4th International Conference on, IEEE, pp. 1-4.

[15] Chen, J., Zhang, F., Mazzaro, L., Lanning, C., Glang, R., Hunter, K., and Shandas, R., "Direct echo PIV flow vector mapping on ultrasound DICOM images," Proc. Ultrasonics Symposium (IUS), 2010 IEEE, IEEE, pp. 1084-1087.

[16] Stewart, K. C., Kumar, R., Charonko, J. J., Ohara, T., Vlachos, P. P., and Little, W. C., 2011, "Evaluation of LV Diastolic Function From Color M-Mode Echocardiography," Journal of the American College of Cardiology: Cardiovascular Imaging, 4(1), pp. 37-46.

[17] Eckstein, A., and Vlachos, P. P., 2009, "Digital particle image velocimetry (DPIV) robust phase correlation," Measurement Science and Technology, 20(5), p. 055401.

[18] Eckstein, A., and Vlachos, P. P., 2009, "Assessment of advanced windowing techniques for digital particle image velocimetry (DPIV)," Measurement Science and Technology, 20(7), p. 075402.

[19] Raben, S. G., Charonko, J. J., and Vlachos, P. P., 2013, "Qi - Quantitative Imaging (PIV and more)," http://sourceforge.net/projects/qi-tools/.

[20] Meinhart, C. D., Wereley, S. T., and Santiago, J. G., 2000, "A PIV algorithm for estimating time-averaged velocity fields," Journal of Fluids Engineering, 122(2), pp. 285-289.

[21] Delnoij, E., Westerweel, J., Deen, N. G., Kuipers, J., and Van Swaaij, W., 1999, "Ensemble correlation PIV applied to bubble plumes rising in a bubble column," Chemical Engineering Science, 54(21), pp. 5159-5171.

[22] Violato, D., and Scarano, F., 2011, "Three-dimensional evolution of flow structures in transitional circular and chevron jets," Physics of Fluids, 23, p. 124104.

[23] Hart, D. P., 2000, "PIV error correction," Experiments in Fluids, 29(1), pp. 13-22.

[24] Keane, R. D., and Adrian, R. J., 1992, "Theory of cross-correlation analysis of PIV images," Applied scientific research, 49(3), pp. 191-215.

[25] Hain, R., and Kähler, C., 2007, "Fundamentals of multiframe particle image velocimetry (PIV)," Experiments in Fluids, 42(4), pp. 575-587.

[26] Charonko, J. J., and Vlachos, P. P., 2013, "Estimation of uncertainty bounds for individual particle image velocimetry measurements from cross-correlation peak ratio," Measurement Science and Technology, 24(6).